

SYNTHESIS, ANALYTICAL AND PHYSICAL DATA OF LIGAND (H₆L) AND ITS METAL COMPLEXES Co(II), Fe(II), Cu(II) AND Ni(II).

Magdy. A. Wasse^{*1}, Abdou. S. EL-Table², Mahmoud. M. Arafa² and Abdullah. A. Alhalib²

^{*1} Department of Chemistry, Faculty of Science, El-Azhar University, Nasr city, Cairo, Egypt.

² Department of Chemistry, Faculty of Science, El-Menoufia University, Shebin El-Kom, Egypt.

Abstract: In this paper we report a systematic study on the synthesis of (H₆L) and its metal complexes: Co(II), Fe(II), Cu(II) AND Ni(II) and characterization as IR frequencies of the bands (cm⁻¹) of ligand and its metal complexes, H¹-NMR analyses, mass spectra, electron spin resonance (ESR).

Keywords: metal complexes, analytical, spectral techniques IR, H¹-NMR, ESR

Introduction :

A series of transition metal complexes with two thiosemicarbazide Schiff bases, 1- (4- dimethyl aminobenzyl- idene) thiosemicarbazide (SBTSC) and 1-(2-pyridin carboxylidene) thiosemicarbazide (PCTSC) were synthesized with Co(II), Ni(II), Zn(II), Cd(II) and Ag(I) salts (chloride and acetate) [1].

Efficient homogeneous catalysts based on ruthenium [2-5], cobalt [2,3], palladium [4-6], copper [7,8] in the process of alcohol oxidation have been reported. Regarding the heterogeneous metal catalysts, mostly gold-palladium [9-11], gold [12], platinum and silver in the forms of nanoparticles, clusters or complexes have been studied as oxidation catalysts. In these articles, the catalyst comprised of a central metal atom and the surrounding organic ligands as well as polyoxometalates typically oxides of molybdenum, tungsten and vanadium are applied for effective oxidation of alcohols [13,14]. For the gas phase oxidation of alcohols, the

suitability of heterogeneous silver catalysts is considered to be the most fit [15,16].

Recently, the applications of monometallic and bimetallic gold based catalysts in the liquid phase of alcohol oxidation were explored in a successful manner [16].

Thiosemicarbazide Schiff base derivatives have considerable anti-bacterial, anti-malarial, anti-viral and anti-tumor activities [17]. Complex ions of such thiosemicarbazide ligands with metal ions are found to produce synergistic effects on antiproliferative activities of the parent ligands.

A series of metal complexes of two thiosemicarbazide Schiff bases with 4-dimethyl aminobenzaldehyde and 2-pyridine carb aldehyde have been synthesized [17].

Metal complex-catalyzed oxidation reactions are quantitatively the most important homogeneously catalyzed reactions in chemical industry [18-20]. In recent years, much work has been dedicated to the search for efficient, selective, environmentally benign and

economic catalytic oxidation processes to ward a sustainable development of chemical processes [21-22].

Experimental:

A. Preparation of the ligand (H₆L)

Hydrazine hydrate (1.43 g ,1mol) was added to 30 cm³ of ethyl alcohol containing sodium salt of p-hydroxy-methyl benzoate (5.0 g , 1mol). Stirring the suspension at 70C° for one hour, The product obtained is filtered off to give a starting material (hydrazide). Glucose in 20 cm³ dissolved in ethyl alcohol was added to the hydrazide heating to 60C° with stirring for an hour. The product obtained was filtered off the yellowish white to yield the ligand (H₆L) as shown below:

Sodium 4-((Z)-2-((2R,3S,4S,5S),2,3,4,5,6pentahydroxyhexylidene)hydrazinecarbonyl)phenolate. Called (H₆L) .

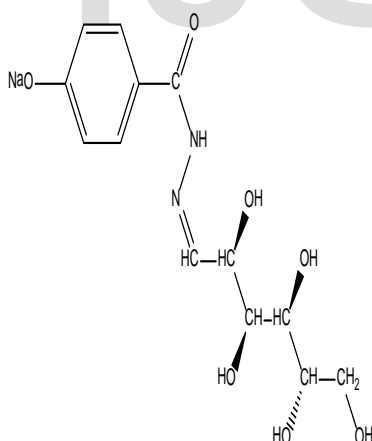


Figure (1) Ligand (H₆L)

B. Preparation of metal complexes:

A) Preparation of [H₅LF₂(SO₄)₂.H₂O]

complex :

iron(II) sulphate tetrahydrate (0.82 g , 1 mol) was added to (H₆L) (1.0 g , 1 mol) dissolved in ethanol 25 cm³. The mixture was warmed at 70 C° with stirring for 1 hour, cool at room temperature and filtered off the dark brown precipitate formed.

B) Preparation of [H₅LCo₂(SO₄)₂.H₂O]

complex :

Cobalt(II) sulphate heptahydrate (0.83 g , 1 mol) was added to (H₆L) (1.0 g , 1 mol) dissolved in ethanol 25cm³. The mixture was warmed at 70 C° with stirring for 1 hour , then cool the mixture at room temperature and then filtered off and the dark brown precipitate was obtained.

C) Preparation of [H₅LCu₂(SO₄)₂.H₂O].H₂O

complex :

Copper(II) sulfate pentahydrate (0.73 g , 1 mol) was added to H₆L (1.0 g , 1 mol) dissolved in ethanol 25cm³. The mixture was warmed at 60 C° with stirring for 1 hour, then the solution was cooled at room temperature filtered off and black precipitate was obtained.

D) Preparation of [H₅LNi₂(SO₄)₂.H₂O]

complex :

Nickel(II) sulfate hexahydrate (0.77 g , 1 mol) dissolved in ethanol 30 cm³ was added to (H₆L) (1.0 g , 1 mol) dissolved in ethanol 25 cm³. The mixture was warmed at 60 C° with stirring for 1 hour, then the solution was

cooled at room temperature filtered off and light brown precipitate was obtained.

E) Preparation of

[H₅LNi₂(OAc)₃.4H₂O].H₂O complex :

Nickle(II) acetate (0.73 g , 1 mol) dissolved in 25cm³ ethanol was added to (H₆L) (1.0 g , 1 mol) dissolved in ethanol 25cm³. The mixture was warmed at 60 C° with stirring for 1 hour, then the solution was cooled at room temperature filtered off and light green precipitate was obtained.

F) Preparation of [H₅LCu₂(OAc)₃.4H₂O].

H₂O complex :

Cobalt(II) acetate tetrahydrate (0.73 g , 1 mol) dissolved in 25 cm³ ethanol was added to (H₆L) (1.0 g , 1 mol) dissolved in ethanol 25 cm³. The mixture was warmed at 60 C° with stirring for 1 hour, then the solution was left at room temperature and when off and dried dark brown precipitate appeared. It was filtered off and at room temperature.

G) Preparation of [H₅LCu₂(OAc)₃.4H₂O].

H₂O complex :

Copper(II) acetate (0.59 g , 1 mol) dissolved in 25cm³ ethanol was added to (H₆L) (1.0 g , 1 mol) dissolved in ethanol 25cm³. The mixture was warmed at 60 C° with stirring for 1 hour, then the solution was cooled at room temperature filtered off the black precipitate which was formed. **Figure (2)**

showed Experimental setup preparation of the ligand and its metal complexes.

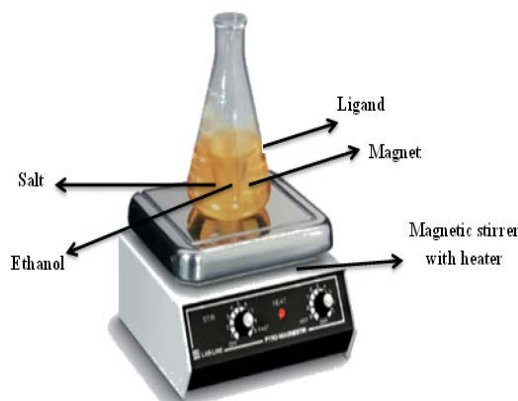


Figure (2) Experimental setup

3) Structural studies of the ligand and its metal complexes

A. Elemental analyses

Elemental analyses (C , H , N and M) were performed by Analytical Laboratory of Al-azhar university , Egypt.

B. Molar conductivity

The molar conductivity of 10⁻³ M of metal complexes in dimethyl-sulfoxide (DMSO) was determined using Bibby conductimeter MCI at room temperature. The molar conductivities were calculated according to the following equation:

$$\Lambda_M = V \cdot K \cdot g / M_w \cdot \Omega$$

Where: Λ_M = molar conductivity (ohm⁻¹ cm² mol⁻¹)

V = volume of the solution (100 cm³)

K = cell constant: 0.92 cm⁻¹

M_w = molecular weight of the complex

g = grams of complex dissolved in 100 cm³ solution

Ω = resistance measured in ohms

C. Mass spectra

The mass spectra of the ligand and its metal complexes were recorded on JEOL JMS-XA- 500 mass spectrometer.

D. Thermal analyses

DTA and TGA were carried out on a Shimadzu DT-30 thermal analyzer in nitrogen atmosphere, from room temperature to 800 C° at a heating rate of 10 C° per minute.

E. ¹H- NMR spectra

The ¹H-NMR spectra were recorded on a JEOL EX -270 MHZ FT- NMR spectrometer in deuterated dimethylsulfoxide (DMSO) as a

solvent. The chemical shifts were measured relative to the solvent peaks.

F- IR spectra

The infrared spectra of solid ligand and its metal complexes were recorded on PerkinElmer's infrared spectrometer 681 using KBr or CsBr discs.

G- ESR spectra

The solid ESR spectra of the complexes were recorded with ELEXSYS E500 Bruker spectrometer in 3 nm Pyrex Tubes at 25 °C. Diphenylpicrylhydrazide (DPPH) free radical was used as a g- marker for the calibration of the spectra. The equation used to determine g- values was :

$$g = (g_{\text{DPPH}}) (H_{\text{DPPH}}) / H$$

Where: $g_{\text{DPPH}} = 2.0036$

H_{DPPH} = magnetic field of DPPH in gauss

H = magnetic field of the sample in gauss

RESULTS AND

DISCUSSION

I. Preparation and investigation of (H₆L) and its complexes:

The elemental analyses, spectral data (Tables 1 and 2) reveal that, the complexes are formed in (1:1) (L:M) stoichiometric ratios. The complexes are colored, stable in air; soluble in polar solvents such as DMF and DMSO and ethanol, CHCl₃ and insoluble in nonpolar solvents such as benzen .

Many attempts were made to grow single crystal, but unfortunately no crystal has been obtained until now. The reaction of ligand with metal ions in ethanol led to the formation of complexes (2)-(8), respectively. The suggested structures of the metal complexes shown in Figure (17 - 23).

Table (1):- Analytical and Physical Data of the Ligand (H₆L) and its Metal Complexes Co(II), Fe(II), Cu(II) and Ni(II).

No.	Ligando/Complexes	Color	FW	MP (°C)	Yield (%)	Anal. /Found(Calc) (%)			Molar conductance*
						C	H	N	
(1)	C ₁₂ H ₁₂ N ₂ O ₂ Na	yellowish white	356	142	70	46.21 (46.43)	4.98 (5.10)	8.0 (8.3)	4.3
(2)	C ₁₂ H ₁₂ N ₂ O ₂ NaCo	Dark brown	661.86	>100	80	23.12 (23.58)	2.23 (2.58)	4.1 (4.23)	17.52 (17.79)
(3)	C ₁₂ H ₁₂ N ₂ O ₂ NaFe	Dark brown	655.7	>100	90	23.32 (23.79)	2.15 (2.59)	4.2 (4.27)	16.82 (17.02)
(4)	C ₁₂ H ₁₂ N ₂ O ₂ NaCu	Black	671.1	>100	60	23.31 (23.24)	2.4 (2.53)	3.98 (4.17)	18.72 (18.93)
(5)	C ₁₂ H ₁₂ N ₂ O ₂ NaNi	Light brown	661.28	>100	70	23.15 (23.58/43)	2.42 (2.57)	4.0 (4.23)	17.12 (17.4)
(6)	C ₁₂ H ₁₂ N ₂ O ₂ NaNi	Light green	587.38	>100	60	32.32 (32.47)	3.32 (3.56)	3.78 (3.98)	16.52 (16.80)
(7)	C ₁₂ H ₁₂ N ₂ O ₂ NaCo	Dark brown	720	>100	80	31.12 (31.67)	4.52 (4.86)	3.65 (3.88)	10.81 (10.46)
(8)	C ₁₂ H ₁₂ N ₂ O ₂ NaCu	Black	671	>100	60	22.80 (23.24)	2.53 (2.53)	3.95 (4.17)	18.72 (18.92)

* Λ_m (Ω⁻¹cm²mol⁻¹)

Table (2):- IR Frequencies of the Bands (cm⁻¹) of Ligand and its Metal Complexes

No.	$\nu(\text{H}_2\text{O})$ (OH)	$\nu(\text{NH})$	$\nu(\text{C}-\text{OH})$	$\nu(\text{C}-\text{O})$	$\nu(\text{C}-\text{N})$	$\nu(\text{Ar})$	$\nu(\text{H}-\text{bond})$	$\nu(\text{O}=\text{C})/(\text{SO}_4)$	$\nu(\text{M}-\text{O})$	$\nu(\text{M}-\text{N})$	$\nu(\text{COOH})_{\text{cont.}}$
(1)	3520-3300	3180	1376,1237	1687	1605	1515,774	3620-3120 3110-2500	-	-	-	-
(2)	3450-3310	3185	1288,1238	1683	1600	1513, 778	3600-3190 3180-2750	1100,1099 860,700	426	560	1360
(3)	3250-3100 3400-3250	3150	1286,1238	1700	1640	1520,770	3550-3100 3200-2800	1162,1098, 850,700	615	570	1350
(4)	3330-3210 3500-3220	3170	1286,1239	1685	1610	1510,774	3610-3180 3170-2700	1167,1020, 853,695	427	558	1380
(5)	3340-3235 3400-3315	3160	1288,1241	1685	1602	1514,773	3620-3210 3200-2800	1157,1102 855,700	432	550	1365
(6)	3500,3420, 3360	3200	1360,1332, 1227	1688	1592	1510,774	3610-3180 3170-2650	1561,1380	436	558	-
(7)	3400,3350, 3300	3220	1287,1238	1685	1585	1430,776	3580,3160 3150-2630	1536,1460 1495,1349	422	582	-
(8)	3450,3400, 3380	3180	1355,1334, 1330	1690	3180	1505,775	3600-3185 3160-2640	1620,1370	640	553	-

A. ¹H-NMR analyses of the ligand (H₆L).

The ¹H-NMR spectrum of the ligand was recorded in deuterated DMSO with Bruker WP 2000 spectrometer operating at 200.13 MHz. Chemical shift are reported with respect to an external tetramethylsilane reference. Table (3) showed ¹H-NMR data of the ligand and spectrum is shown in Figure (3).

Table (3): ¹H-NMR data for the ligand (H₆L).

Ar	NH	CHOH	CH ₂ OH	CHN
6.8-8.0	5.0	3.5-4.3	3.3	2.5

*Chemical shift (δ) ppm .

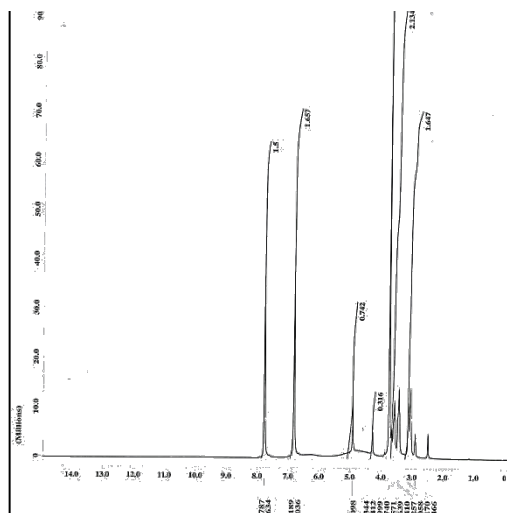


Figure (3) H¹NMR data for the ligand

B. Mass spectra:

The mass spectrum of the free ligand, Table (4) and Figure (4,5) revealed a molecular ion peak (m/z) at 338 a.m.u which is coincident with the formula weight of the ligand and supports the identity of the Structure. Furthermore, the fragments observed at m/z = 53, 62, 85, 101, 104, 145, 267, 297, 313 and 336 corresponding to CH₃O₂, C₂H₆O₂, C₃H₁O₃, C₄H₅O₃, C₄H₈O₃, C₅H₅O₅, C₁₃H₁₇N₂O₄, C₁₃H₁₇N₂O₆, C₁₃H₁₇N₂O₇, and C₁₃H₁₇N₂O₇Na moieties respectively.

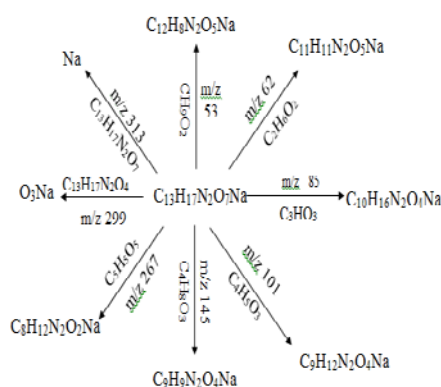


Figure (4) mass spectra of the Ligand(H₆L)

Table (4):- Mass spectrum of the ligand(H₆L).

m/z	Rel. Int.	Assignments
53	19	(CH ₃ O ₂)
62	14	(C ₂ H ₆ O ₂)
85	7	(C ₃ H ₁ O ₃)
101	100	(C ₄ H ₅ O ₃)
104	8	(C ₄ H ₈ O ₃)
145	6	(C ₅ H ₅ O ₅)
267	9	(C ₁₃ H ₁₇ N ₂ O ₁₂)
297	16	(C ₁₃ H ₁₅ N ₂ O ₁₃)
313	28	(C ₁₃ H ₁₅ N ₂ O ₇)
336	8	(C ₁₃ H ₁₇ N ₂ O ₇ Na)

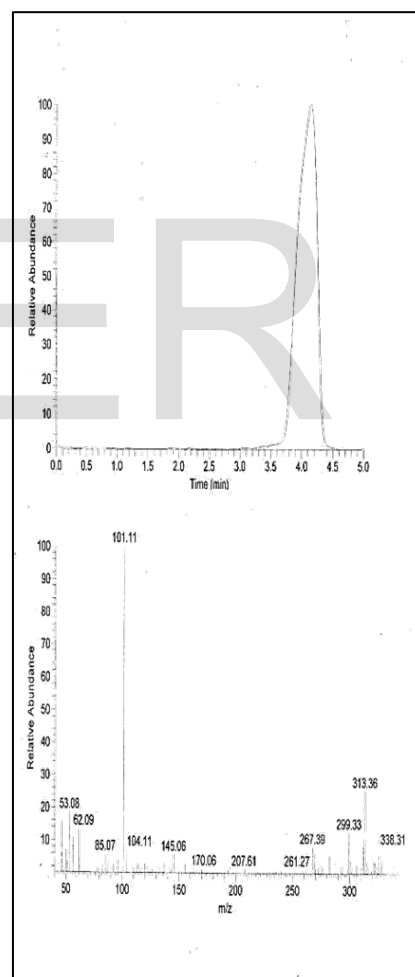


Figure (5) Mass spectrum of the ligand (H₆L)

C. Conductivity

The molar conductivity of 1×10^{-3} M solution of the ligand and metal complexes (**1**)-(**8**) in DMSO at room temperature are given in (**Table 1**). The value of molar conductance of all complexes are in the $4.3\text{-}14.21 \text{ } \Omega^{-1}\text{cm}^2 \text{ mol}^{-1}$ range (**Table 1**), indicating a non-electrolytic nature of these complexes,[23] confirming the involvement of the acetate, sulfate, nitrate and chloride anions in the coordination sphere.

D. Infrared spectra

Important spectral bands of the ligand and its metal complexes are presented in **Table (2)**. The IR spectrum of the ligand showed broad medium intensity bands in the $3630\text{-}3120$ and $3110\text{-}2500 \text{ cm}^{-1}$ ranges, which are attributed to intra- and intermolecular hydrogen bondings. The broad medium bands at 3520 and 3300 cm^{-1} are assigned to the OH groups, whereas the relatively strong bands located at 1376 and 1237 cm^{-1} , is assigned to the $\nu(\text{COH})$.

Tetrabasic multidentate ligand: coordinating through enolic oxygen[24], imine ($\text{C}=\text{N}$) and ($\text{>C}=\text{O}$) groups. This mode of coordination is supported by (i) vibration band of the ($\text{C}=\text{N}$) was shifted to lower wave number with a decreasing its intensity while the other one band appeared in its original place. (ii) The appearance of new bands in the 590 and 619 cm^{-1} regions are due to the $\nu(\text{M-N})$ and $\nu(\text{M-O})$ vibrations respectively.

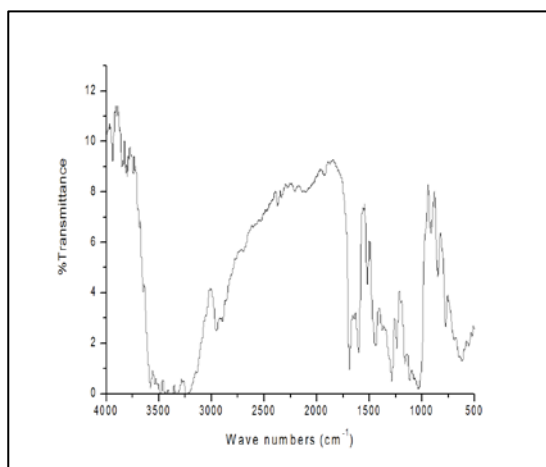
(iii) The strong bands observed around 1650 and 1630 cm^{-1} , characteristic to the carbonyl ($\text{C}=\text{O}$) stretching vibrations were shifted to lower wave numbers, suggesting coordination of the carbonyl oxygen atoms to the metal ion.

The presence of water molecules within the coordination sphere in all complexes were supported by the presence of weak bands around $3500\text{-}3310 \text{ cm}^{-1}$ due to OH stretching, H_2O deformation, H_2O rocking and H_2O wagging, respectively. The appearance of two characteristic bands in the $1160\text{-}1099$ and $860\text{-}700$ and $1620\text{-}1370 \text{ cm}^{-1}$ ranges in the spectra of complexes, were attributed to $\nu(\text{COO}^-)$, $\nu_{\text{asym}}(\text{COO}^-)$ and $\nu_{\text{sym}}(\text{COO}^-)$ respectively, indicating the participation of the acetate oxygen in the complex formation [25].

The coordination modes of the acetate group in the complexes were determined by IR spectra, by comparing the separations between the $\nu_{\text{asym}}(\text{COO}^-)$ and $\nu_{\text{sym}}(\text{COO}^-)$. The separation value (Δ) between $\nu_{\text{asym}}(\text{COO}^-)$ and $\nu_{\text{sym}}(\text{COO}^-)$, suggesting a tridentate coordination fashion of the acetate groups **complex (2-8)** [26].

Complexes spectra demonstrated strong to medium bands at $1167\text{-}1020$ and $853\text{-}695 \text{ cm}^{-1}$ belonging to the antisymmetric and symmetric stretching modes of the sulfate group. These values are consistent with that reported for the sulfate species coordinating to the Cu(II) in an tridentate fashion. The spectra

of the ligands and their metal complexes are shown in **Figures (6 - 13)**. [27]



Figure(6): IR spectrum of the ligand (H₆L)

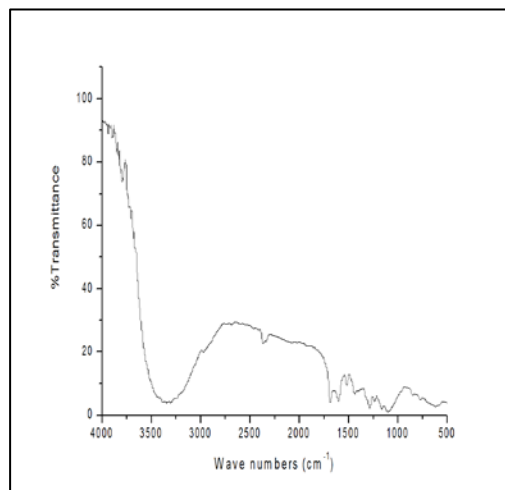


Figure (8): IR spectrum of [H₅LFe₂(II)(SO₄)₂.H₂O] complex (3)

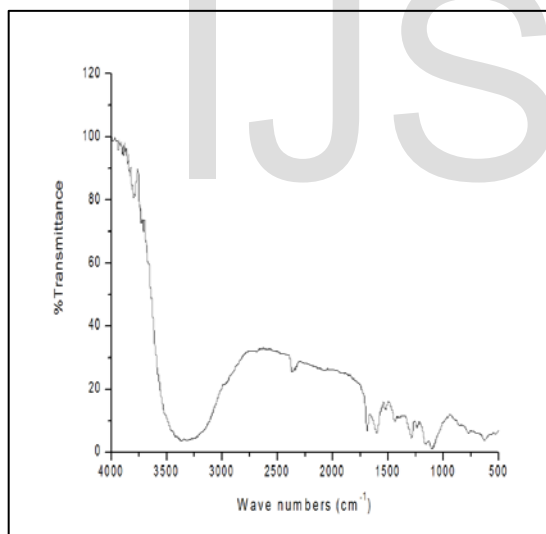


Figure (7): IR spectrum of [H₅LCo₂(II)(SO₄)₂.H₂O] complex (2)

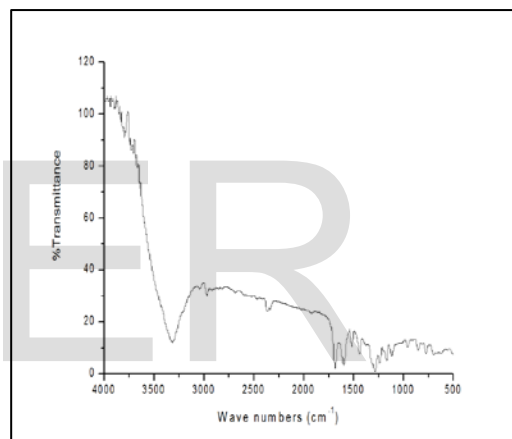


Figure (9): IR spectrum of [H₅LCu₂(II)(SO₄)₂.H₂O].H₂O complex (4)

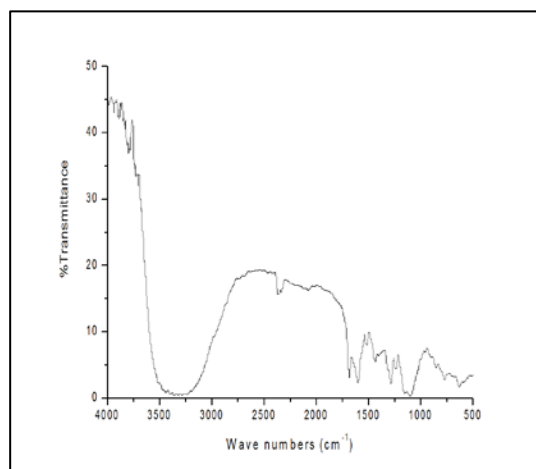


Figure (10): IR spectrum of [H₅LNi₂(II)(SO₄)₂.H₂O] complex (5)

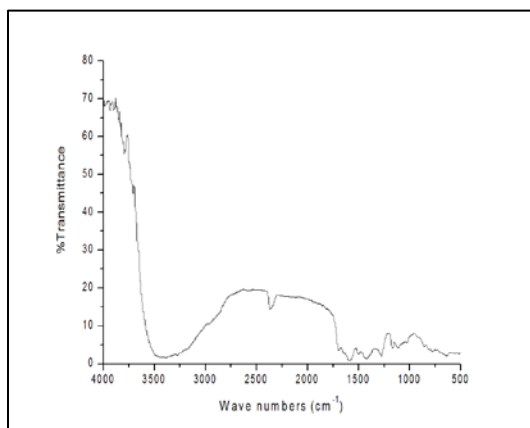


Figure (11): IR spectrum of [HsLNi(II)(OAc)₃.4H₂O].H₂O complex (6)

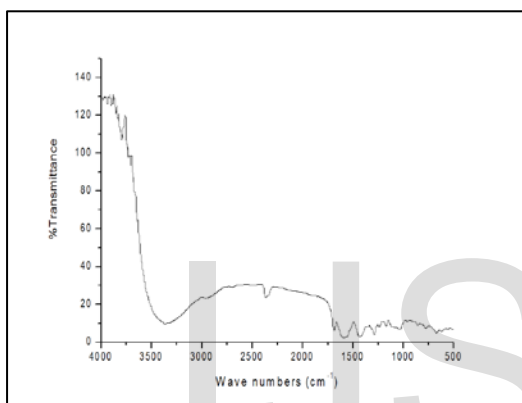
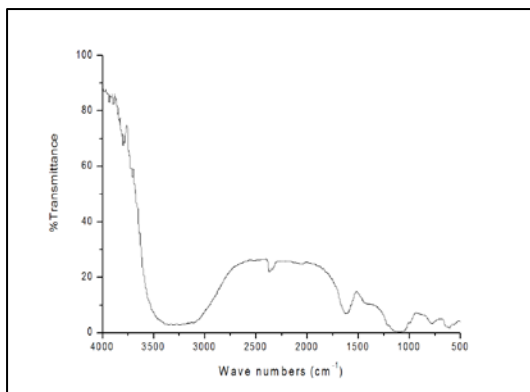


Figure (12): IR spectrum of [HsLCo₂(II)(OAc)₃.4H₂O].H₂O complex (7)



Figure(13): IR spectrum of [HsLCu₂(II)(OAc)₃.4H₂O].H₂O complex (8)

E. Electronic spectra and magnetic moments

DMF electronic absorption spectral bands as well as room temperature effective magnetic moment values of the ligand and its metal complexes are reported in **Table 5**. The ligand showed three transition bands in the high energy region. The first band appeared at 270 nm which is assigned to $\pi \rightarrow \pi^*$ transition within the aromatic rings and this band is nearly unchanged upon complexation. The second and third bands appearing at 295 and 315 nm may be assigned to $n \rightarrow \pi^*$ of the azomethine group and CT transitions.

The bands were found to be shifted upon complexation indicating involvement of these bands in coordination with the metal ions. The electronic spectra of the Co(II) complexes **(2)** and **(7)** exhibit three transition bands at 435, 530 and 600 nm ${}^4T_{1g}(F) \rightarrow {}^4T_{2g}(F)$ and 435, 550 and 615 nm respectively. These bands are assigned to ${}^4T_{1g}(F) \rightarrow {}^4T_{2g}(F)$ transitions respectively, corresponding to high spin cobalt(II) octahedral complexes[27]. The magnetic moments of complexes **(2)** and **(7)** are 3.32 and 3.21 BM, which are well within the reported range of high spin octahedral Co(II) complexes. The low value indicates spin-spin interaction takeplace between Co(II) ions. The electronic absorption spectra of Ni(II) complexes **(5)** and **(6)** displayed three bands at 435, 560, and 600 nm and 425, 590, and 605 nm. These bands are corresponding to ${}^3A_{2g}(F) \rightarrow {}^3T_{1g}(F)$ and ${}^3A_{2g}(F) \rightarrow {}^3T_{2g}(F)$ transitions respectively, indicating octahedral nickel(II) complexes[28].

The magnetic moment values of nickel(II) complex **(5)** and **(6)** 2.35 and 2.28 BM,

which are consistent with two unpaired electrons state and confirming octahedral geometry around nickel(II) ions [28]. The low value indicates spin-exchange interaction take place between Ni(II) ions. The electronic spectra of copper(II) complexes (4) and (8) exhibited bands in the 605 and 615 nm which are assigned to ${}^2B_{1g} \rightarrow {}^2A_{1g}$ ($d_{x^2-y^2} \rightarrow d_{z^2}$), and ${}^2B_{1g} \rightarrow {}^2E_g$ ($d_{x^2-y^2} \rightarrow d_{xy}, d_{yz}$) transitions respectively. These transitions indicate that, the copper(II) ion has a tetragonally distorted octahedral geometry [28]. This could be due to the Jahn-Teller effect that operates on the d^9 electronic ground state of six coordinate system, elongating one trans pair of coordinate bonds and shortening the remaining four ones.

Copper(II) complexes (4) and (8) show magnetic moment values are 1.55 and 1.52 BM, which are consistent with octahedral geometry around the copper(II) ion. Diamagnetic Iron(II) complex (3) showed only intraligand transitions and LMCT.

Table (5):- Electronic Spectra (nm) and Magnetic Moments (B.M) for the Ligand and its metal Complexes.

Comp. No.	λ_{max} (nm)	μ_{eff} (BM)
(1) ligand	270,295,315	-
(2)	270,285,310,435,530,600	3.32
(3)	270,290,300,415,535,612	Diamagnetic
(4)	270,285,305,440,565,605	1.55
(5)	270,282,303,435,560,600	2.35
(6)	270,280,300,425,590,605	2.28
(7)	270,282,303,435,550,615	3.21
(8)	270,285,300,435,528,615	1.52

1

F. Electron spin resonance (ESR)

The ESR spectral data for metal complexes (2), (4) and (8) are presented in Table (6). The spectra of copper(II) complexes (4) and (8) are characteristic of species, d^9 , configuration and having axial type of a $d(x^2-y^2)$ ground state which is the most common for copper(II) complexes. The metal complexes showed $g_{||} > g_{\perp} > 2.03$, indicating octahedral geometry around the copper(II) ion. The expression G is related to g-values, $G = (g_{||}-2)/(g_{\perp}-2)$. If $G > 4.0$, then local tetragonal axes are misaligned parallel or only slightly misaligned and if $G < 4.0$, significant exchange coupling is present.

Metal complexes showed values indicating spin-exchange interactions take place between the copper(II) ions, which is consistent with the magnetic moments values (Table 6). Also, the $g_{||}/A_{||}$ values are considered as a diagnostic of stereochemistry. The $g_{||}/A_{||}$ values lie just within the range expected for the octahedral metal complexes. The orbital reduction factors ($K_{||}$, K_{\perp} , K), which are a measure of covalence were also calculated. K values, for the copper(II) complexes, indicating covalent bond character. Also, the g-values show considerable a covalent bond character.

The in-plane σ -covalency parameter, α^2 (Cu) suggests a covalent bonding. The complexes show β_1^2 values indicating a covalency character in the in-plane π -bonding. While β^2 for the complexes indicating a covalent bonding character in the out of plane π bonding except complexes which indicate ionic bond character. The calculated orbital

populations (a^2_d) for the copper(II) complexes indicate a $d(x^2-y^2)$ ground state. Complex (2), show isotropic spectra. The ESR spectra of complexes (2), (4) and (8) are shown in Figures (14-16)

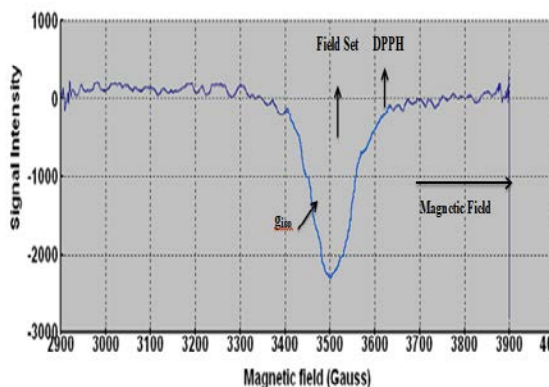


Figure (14): ESR spectrum of Co(II) complex (2)

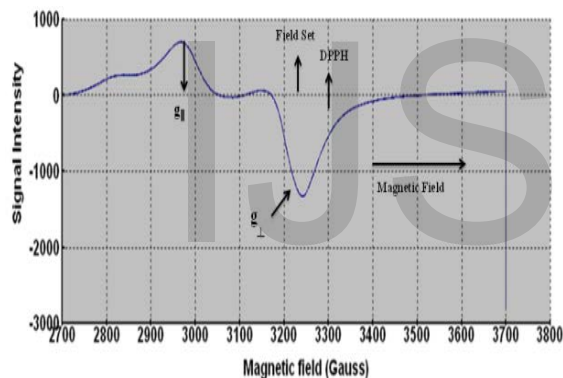


Figure (15): ESR spectrum of Cu(II) complex (4)

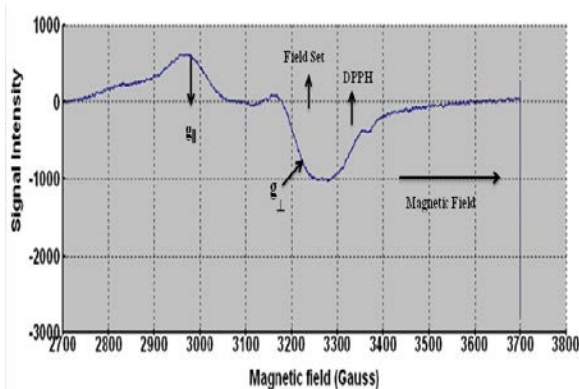


Figure (16): ESR spectrum of Cu(II) complex (8)

Table (6): ESR data for the metal complexes.

No. Of complex	g_{\parallel}	g_{\perp}	g_{iso}^a	A_{\parallel} (G)	A_{\perp} (G)	A_{iso}^b (G)	G^c	ΔE_{xy} (cm ⁻¹)	ΔE_{xz} (cm ⁻¹)	K_1^2	K_2^2	K	$g_{\parallel}/A_{\parallel}$ (cm ⁻¹)	α^2	β^2	β_1^2
(2)	-	-	2.04	-	-	-	-	-	-	-	-	-	-	-	-	-
(4)	2.19	2.05	2.09	120	15	50	3.8	16529	22727	0.66	0.46	0.77	182.5	0.47	1.44	0.97
(8)	2.21	2.08	2.0	130	17.5	55	3.5	16260	22988	0.8	0.51	0.83	170	0.63	1.27	0.81

a) $3g_{iso} = g_{\parallel} + 2g_{\perp}$

b) $3A_{iso} = A_{\parallel} + 2A_{\perp}$

c) $G = (g_{\parallel} - 2)/(g_{\perp} - 2)$

Reference:

1. M. Tayebani, B. Shafaat, M. Iravani. Iranian Journal of Catalysis; (2015), 5(3), 213.
2. M.L. Kantam, U. Pal, B. Sreedhar, S. Bhargava, Y. Iwasawa, M. Tada and B.M. Choudary ; Adv. Cat. (2008) ,350 ,1225.
3. M. J. Jacinto, O.H. Santos, R.F. Jardim, R. Landers and L.M. Rossi ; Appl. Catal. A: Gen (2009) , 360 , 177.
4. A. Kockritz, M. Sebek, A. Dittmar, J. Radnik, A. Bruckner, U. Bentrup, M.M. Pohl, H. Hugel and W. Magerlein ; J. Mol. Catal. A: Chem. (2006) , 246 , 85 .
5. M. Hasan, M. Musawir, P.N. Davey and I.V. Kozhevnikov ; J. Mol. Catal. A: Chem. (2002) ,180 ,77 .
6. J. Chen, Q. Zhang, Y. Wang and H. Wan ; Adv. Catal.(2008) , 350 ,453 .
7. A. Villa, N. Janjic, P. Spontoni, D. Wang, D.S. Su and L. Prati ; Appl. Catal. A: Gen (2009) , 364 , 221 .
8. C.Y. Ma, B.J. Dou, J.J. Li, J. Cheng, Q. Hu, Z.P. Hao and S.Z. Qiao ; Appl. Catal. B: Envi. (2009) , 92 , 202 .
9. P.G.N. Mertens, P. Vandezande, X. Ye, H. Poelman, D.E. De Vos and I.F. Vankelecom ; Adv. Catal. (2008) , 350 , 1241 .
10. P. Haider, B. Kimmerle, F. Krumeich, W. Kleist, J.D. Grunwaldt and A. Baiker ; Catal. Lett. (2008) , 125 , 169.

11. M. Ilyas and M. Sadiq ; Chem. Eng. Tech. **(2007)**, 35 , 1391.
12. M.J. Beier, T.W. Hansen and J.D. Grunwaldt ; J. Catal. **(2009)** 320.
13. Y. Sawayama, H. Sibahara, Y. Ichihashi, S. Nishiyama and S.Tsuruya ; Ind. Eng. Chem. Res. **(2006)** , 45 , 8837.
14. J. Shen, W. Shan, Y. Zhang, J. Du, H. Xu, K. Fan, W. Shen and Y. Tang ; J. Catal. **(2006)** , 237 , 94.
15. W.C. Ketchie, M. Murayama and R. Davis ; Top. Catal. **(2007)** , 44 , 307.
16. W.C. Ketchie, Y.L. Fang, M.S. Wong, M. Murayama and R. J. Davis ; J. Catal. **(2007)** , 250 , 264.
17. Z. Xu, Z. Kong, S. Sun and X. Wang ; Acta Crystallogr. Sect. A: Fou. **(2009)** , 65 , 273.
18. U. Encyclopedia ; Indus. Chem. **(2002)**.
19. R. Whyman, App. Organo. Chem. Cat. **(2001)** .
20. R.A. Smiley and H.L Jackson ; Chem. and the Chem. Indu. **(2002)**.
21. R.A. Sheldon, I. Arends and U. Hanefeld ; Gre. Chem. and Cata. **(2007)** .
22. G.P. Chiusoli and P.M. Maitlis ; Roy. Soc. of Chem. Camb. **(2006)** (Chap. 2, 4).
23. A. S. El-tabl ; polish J .Chem. **(2000)** , 73,1937.
24. P. Deveci , B.Taner , Z.kilic , A.O. solak , U.Arslan , E.Ozcan ; Polyhedron. **(2011)** , 30 , 1726.
25. B. Marukan , K. Mohanan ; Tran. met. Chem. **(2006)** , 31 , 441.
26. A. S. El-tabl , F. A. Elsaied , A. N. Alhakimi ; Syn. Tran. Met. **(2007)** , 32 , 89.
27. Z. H. Chohan , C. T. Supuran ; App. Orga. Chem. **(2005)** , 19 , 1207.
28. H. G. Aslan , S. Ozcan , N. Karakan , Ino. Chem. Com. **(2011)** , 14 , 1207.

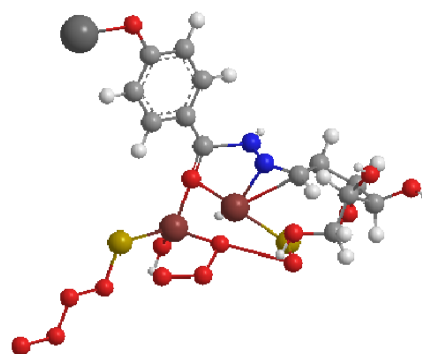
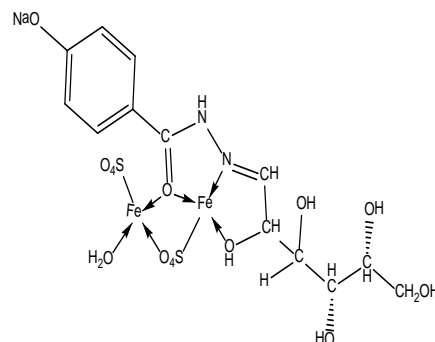


Figure (17) $[H_5LFe_2(SO_4)_2.H_2O]$ complex and

3D structure

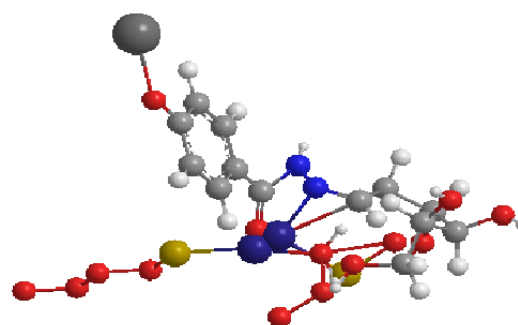
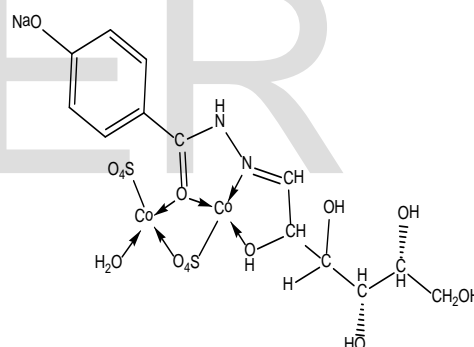


Figure (18) $[H_5LCo_2(SO_4)_2.H_2O]$ complex and

3D structure

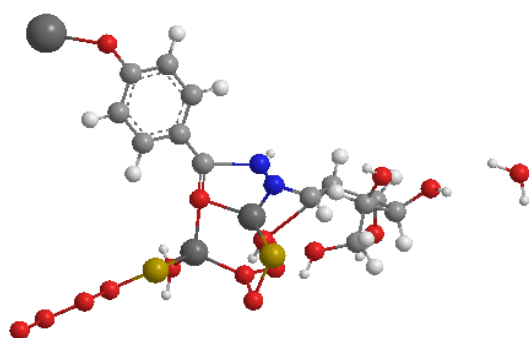
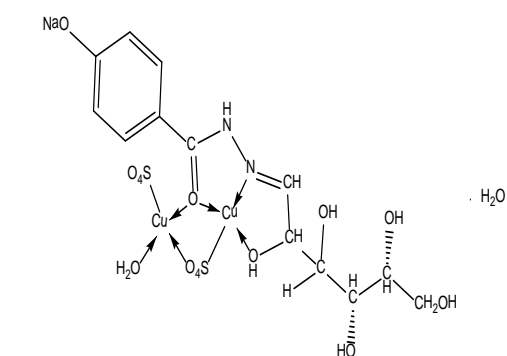


Figure (19) $[H_5LCu_2(SO_4)_2.H_2O].H_2O$ complex and 3D structure

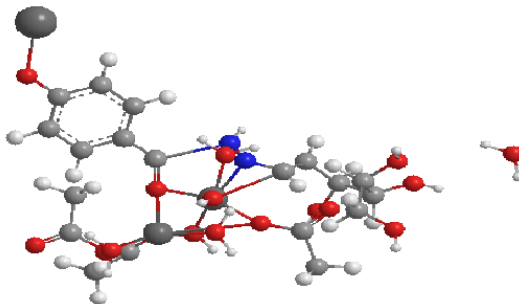
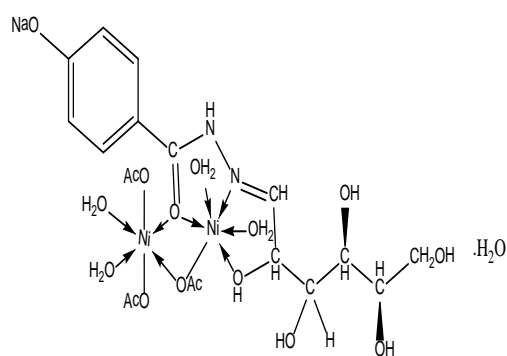


Figure (21) $[H_5LNi_2(OAc)_3.4H_2O].H_2O$ complex and 3D structure

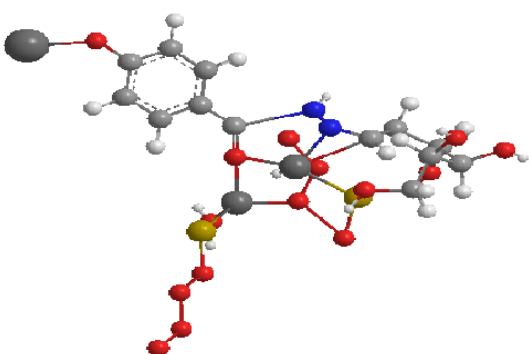
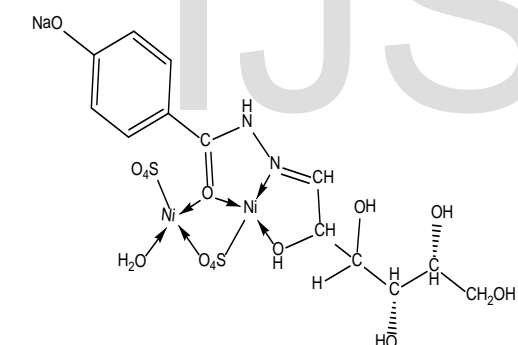


Figure (20) $[H_5LNi_2(SO_4)_2.H_2O]$ complex and 3D structure

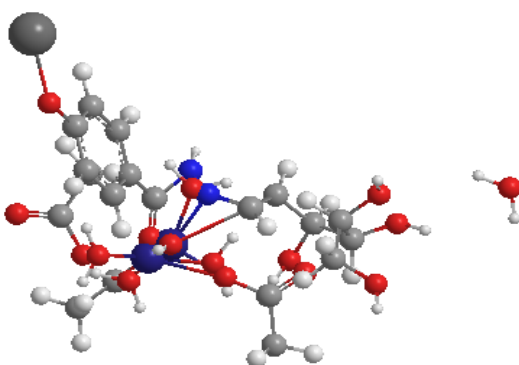
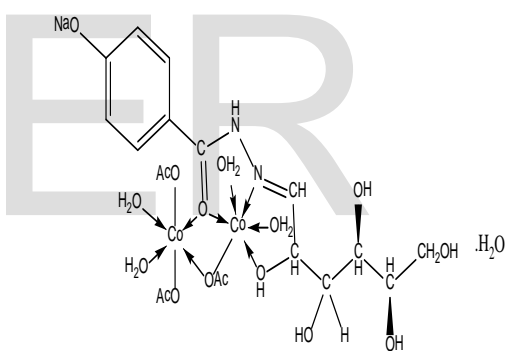
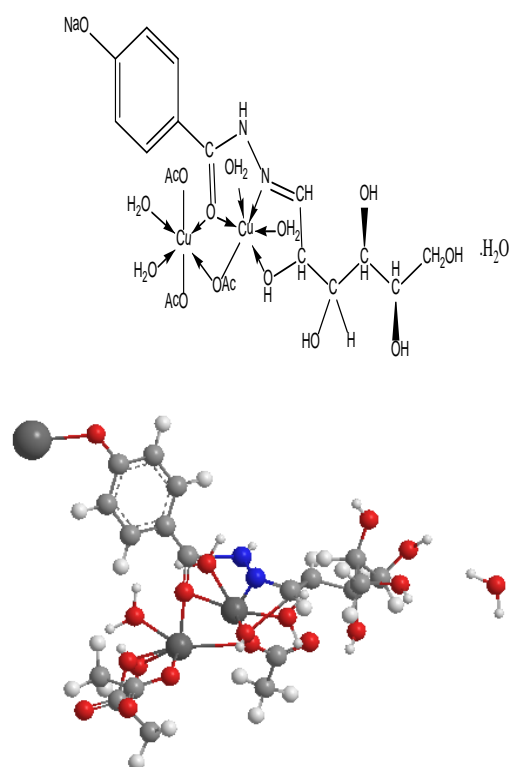


Figure (22) $[H_5LCo_2(OAc)_3.4H_2O].H_2O$ complex and 3D structure



**Figure (23) $[H_5LCu_2(OAc)_3 \cdot 4H_2O] \cdot H_2O$
complex and 3D structure**

IJSER